Evaluation of computational techniques for solving the Boltzmann transport equation for lattice thermal conductivity calculations

Aleksandr Chernatynskiy* and Simon R. Phillpot
Department of Materials Science and Engineering, University of Florida, Gainesville, Florida 32611, USA
(Received 7 June 2010; published 4 October 2010)

Three methods for computing thermal conductivity from lattice dynamics (the iterative method, the variational method, and the relaxation-time approximation) are compared for the prototypical case of solid argon. The iterative method is found to produce results in close agreement with Green-Kubo molecular-dynamics simulations, a formally correct method for computing thermal conductivity. The variational method and relaxation-time approximation are found to underestimate the thermal conductivity. The relationship among the methods is established; a combination of the iterative and variational methods is found to have a fastest convergence. Formal convergence of the iterative method is demonstrated and a simple mixing rule is shown to provide stability in practice. The ability to use these methods to provide detailed insight into the relationship between phonon properties and thermal conductivity is demonstrated.

DOI: 10.1103/PhysRevB.82.134301 PACS number(s): 44.05.+e, 63.20.kg

I. INTRODUCTION

Fast and reliable prediction of the thermal conductivity of electrical insulators remains a challenge. The direct nonequilibrium molecular-dynamics (MD) method and the equilibrium Green-Kubo (GK) approach both suffer from the long simulation times and significant size effects.[1] These make it impossible to couple them to first-principles molecular-dynamics methods while classical empirical and semiempirical potentials may not display sufficiently high materials fidelity. At the same time, the development of the perturbation theory within density-functional theory allows the third-order force-constant matrices to be determined without resorting to the numerical differentiation.[2] This has revitalized interest in lattice dynamics methods to solve the Boltzmann transport equations (BTE) for phonons. There are three major approaches for the approximate solution of the (BTE): the relaxation-time approximation,[3,4] the variational approach,[5–8] and the iterative method.[9,10] Each method has potential advantages and drawbacks. The main drawback of the relaxation-time approximation is that it is not intrinsically controlled, thus making it difficult to quantify errors in the method, or to systematize improvements to it. In practice, however, results from the relaxation-time approximation compare very favorably with experiment. In the relaxation-time approximation, one is not limited to lattice dynamics for computing phonons relaxation times, which may also be calculated by molecular-dynamics methods; thus the relaxation-time approximation can account for the full anharmonicity of the system. An important advantage of the variational approach is that, in contrast to the relaxation-time approximation, it is intrinsically a controlled approximation to the correct solution, always producing a lower bound for the thermal conductivity. However, there are no systematic approaches for the development of high-quality variational functions. Various variational functions were investigated by Pettersson;[8] the quality of these variation functions, and others, will be assessed here. The iterative method is the most recent technique.[9] Its main advantage is that it enables the numerical solution of the linearized Boltzmann equation without resort to any prescribed form of the solution, as required by the relaxation-time approximation or variational principle. Its main disadvantage is that it typically requires an order of magnitude longer computational time.

In this paper, we compare the performance the three approaches against each other, establish the connections among different methods, and present technical details of their implementations. A simple representative problem is considered: the thermal conductivity of a solid argon, a classic case investigated in a detail previously by both lattice dynamics[4,9] and various molecular-dynamics techniques.[4,11–15]

The paper is organized in the following way. A brief description of the theory is presented in Sec. II; validation of our implementations of the various methods is given in Sec. III. The results obtained by the various methods are compared with each other and with molecular-dynamics results in Sec. IV. Section V contains our conclusions. A more detailed description of BTE and solution methods is presented in the Appendix A. Details of the application of BTE to phonons are given in Appendix B while tech nical details of our implementations are given in Appendix C.

II. THEORY

In this section we briefly outline the various methods for the calculation of the thermal conductivity from lattice dynamics. The appendices contain a full description of the theory, including the technical details of the implementation. The three methods that we discuss in this paper (variational, iterative, and relaxation-time approximation methods) are concerned with the solution of the canonical form of the linearized BTE for phonons [see Eq. (A10)]

$$-\vec{v}_{\vec{k},n}\cdot\frac{\partial f^0_{\vec{k},n}}{\partial T}\nabla T=\frac{1}{k_BT}\left\{\sum_{\vec{k}',n';\vec{k}'',n''}\left[(\Phi_{\vec{k},n}+\Phi_{\vec{k}',n'}-\Phi_{\vec{k}'',n''})\Lambda^{\vec{k}'',n''}_{\vec{k},n;\vec{k}',n'}+\frac{1}{2}(\Phi_{\vec{k},n}-\Phi_{\vec{k}',n'}-\Phi_{\vec{k}'',n''})\Lambda^{\vec{k}',n';\vec{k}'',n''}_{\vec{k},n}\right]+\cdots\right\}. \quad (1)$$

In this expression, the branch index n and the reciprocal vector $\vec{k}$ label phonon states, $\vec{v}_{\vec{k},n}$ is the group velocity of the phonon; $f^0_{\vec{k},n}$ is the equilibrium Bose-Einstein distribution; T is the temperature; k_b is a Boltzmann constant; $\Phi_{\vec{k},n}$ is the unknown perturbation to the distribution function associated with the steady-state, nonequilibrium conditions caused by temperature gradient, ∇T; and Λ is the equilibrium transition rates for a specific process. In this approximation, Λ includes only three-phonon processes; such three-phonon processes are well known to be the dominant process associated with the intrinsic conductivity; however, four-body and higher body processes can also contribute to the thermal conductivity. The appropriateness of this approximation and the magnitude of the contributions from the higher order processes are assessed in Sec. IV. We begin by briefly outlining the three processes.

A. Iterative method

The iterative method starts from Eq. (1). By rearranging the terms, an iterative process is set up (see Appendix A)

$$\vec{F}^{i+1}_{\vec{k},n}=\vec{F}^0_{\vec{k},n}+\frac{1}{Q_{\vec{k},n}}\int\int\sum_{n'n''}\left[(\vec{F}^i_{\vec{k}'',n''}-\vec{F}^i_{\vec{k}',n'})\Lambda^{\vec{k}'',n''}_{\vec{k},n;\vec{k}',n'}+\frac{1}{2}(\vec{F}^i_{\vec{k}',n'}+\vec{F}^i_{\vec{k}'',n''})\Lambda^{\vec{k}',n';\vec{k}'',n''}_{\vec{k},n}\right]d\vec{k}'\,d\vec{k}'' \quad i=1,2,3\ldots. \quad (2)$$

The iterative process is launched with an initial condition

$$\vec{F}^0_{\vec{k},n}=-\frac{f^0_{\vec{k},n}(1+f^0_{\vec{k},n})\vec{v}_{\vec{k},n}}{TQ_{\vec{k},n}},\quad \vec{F}^1_{\vec{k},n}=0. \quad (3)$$

In this initial condition each mode behaves as if all other modes are in equilibrium, which is equivalent to the relaxation-time approximation discussed below. In these expressions, $\vec{F}_{\vec{k},n}$ is a proxy for the distribution-function perturbation

$$\Phi_{\vec{k},n}=\vec{F}_{\vec{k},n}\cdot\nabla T. \quad (4)$$

Physically, this representation is consistent with assumption the linear-response theory underlying Fourier's law. In Eq. (3), quantity $Q_{\vec{k},n}$ is defined as

$$Q_{\vec{k},n}=\int\int\sum_{n'n''}\left[\Lambda^{\vec{k}'',n''}_{\vec{k},n;\vec{k}',n'}+\frac{1}{2}\Lambda^{\vec{k}',n';\vec{k}'',n''}_{\vec{k},n}\right]d\vec{k}'\,d\vec{k}''. \quad (5)$$

As we will see shortly, $Q_{\vec{k},n}$ is inversely proportional to the single-mode relaxation time. The thermal conductivity is calculated from Fourier's law using the standard expression for the heat current in terms of the distribution function [Eq. (A19)]

$$k=-\int\sum_n\hbar\omega_{\vec{k},n}\frac{f^0_{\vec{k},n}(1+f^0_{\vec{k},n})}{k_BT}\vec{v}_{\vec{k},n}\otimes\vec{F}^i_{\vec{k},n}d\vec{k}. \quad (6)$$

The iteration scheme is terminated once the difference between values of function $\vec{F}_{\vec{k},n}$ on two consecutive steps is below the specified accuracy level (alternatively, one can use convergence in the thermal-conductivity values). The steps in the calculation using the iterative method are completely deterministic. Convergence of the series can be established since the iterative procedure can be viewed as an implementation of a steepest descent algorithm for the solution of the set of linear equations. In particular, the matrix representing this set of equations is positive definite and symmetric (as shown in Appendices A and B), thus satisfying all the necessary conditions for convergence of the steepest descent algorithm. The result of the iterative process is an estimate of the thermal conductivity of the system, again within the approximation of three-phonon processes only. Higher order phonon processes could be added; however, each additional order would involve an additional integration over the Brillouin zone. While possible, in principle, addition of such higher order terms pushes the limits of practicability since the double integration associated with the cubic terms is already one of the computational bottlenecks in these methods. The other bottleneck is the computation of the third-order dynamical matrices.

B. Variational method

The variational principle for the Eq. (1), see Appendices A and B, asserts the existence of a functional, $\Phi_{\vec{k},n}$, that reaches its minimum for the perturbation, Φ, that is the exact solution to the BTE. The thermal conductivity, in turn, can be represented in terms of such a functional as

$$\frac{1}{k} = \frac{1}{2k_B T^2} \frac{8\pi^3 \hbar^3}{V} \min \left\{ \frac{\int\int\int \sum_{nn'n''} [(\Phi_{\vec{k};n} + \Phi_{\vec{k}';n'} - \Phi_{\vec{k}'';n''})^2 \Lambda^{\vec{k}'';n''}_{\vec{k};n\vec{k}';n'}] d\vec{k} d\vec{k}' d\vec{k}''}{\left(\int \sum_n \vec{v}_{\vec{k};n} \cdot \frac{\partial f^0_{\vec{k};n}}{\partial T} \Phi_{\vec{k};n} d\vec{k} \right)^2} \right\}, \tag{7}$$

The value of $1/k$, therefore, reaches its minimum for the $\Phi_{\vec{k},n}$ that is the solution of the Eq. (1); thus any estimate of k from the variational method is a maximum, at least within the three-phonon approximation. There are two possible approaches to calculating k from the variational approach. In the first approach, one can pick a candidate form for $\Phi_{\vec{k},n}$, based on analysis or intuition, and then calculate the thermal conductivity from Eq. (7). In the second approach, $\Phi_{\vec{k},n}$ can be represented as a linear combination of a chosen basis; Eq. (7) is then minimized with respect to the coefficients of the expansion. Both of these approaches will be analyzed below.

C. Relaxation-time method

The relaxation-time approximation assumes that for small deviations from equilibrium, the rate at which the distribution function for each mode returns to equilibrium is proportional to the deviation from equilibrium, with some relaxation time, regardless of whether other modes are in equilibrium or not

$$-\vec{v}_{\vec{k},n} \cdot \frac{\partial f^0_{\vec{k},n}}{\partial T} \nabla T = \frac{f_{\vec{k},n} - f^0_{\vec{k},n}}{\tau_{\vec{k},n}}. \tag{8}$$

This approach encapsulates all the phonon-scattering physics into the mode relaxation time $\tau_{\vec{k},n}$. Thus this method can be viewed as a generalization of the classic kinetic-theory approach for thermal conductivity. The relaxation time, the inverse of the linewidth of the phonon state, can be determined using many-body perturbation theory.[4,16] Again using the expression for the heat current and Fourier's law, the thermal conductivity is then calculated as

$$k = \int \sum_n (\hbar \omega_{\vec{k},n})^2 \frac{f^0_{\vec{k},n}(1 + f^0_{\vec{k},n})}{k_B T^2} \vec{v}_{\vec{k},n} \otimes \vec{v}_{\vec{k},n} \tau_{\vec{k},n} d\vec{k}. \tag{9}$$

Interestingly, there is an intimate connection between iterative method and relaxation-time approximation. Comparing Eqs. (6) and (9) one can see that the relaxation time can be formally defined in the iterative scheme as

Using the expression for the $\vec{F}^0_{\vec{k},n}$ from Eq. (3), a little algebra yields an expression for the relaxation time that is identical to the one derived from many-body perturbation theory (Eq. 16 in Ref. 4). Thus, the relaxation-time approximation is formally identical to the first step in the iterative procedure. Subsequent iterations give ever more precise solutions to the BTE.

Computation of the integrals in Eq. (2) is generally straightforward, with the only major difficulty being the handling of the energy δ function that enters transition rates Λ. We choose to use the approach proposed by Pettersson;[7] details of this computation are presented in Appendix C. In this approach, the energy δ function is taken into account analytically, thus reducing the inner integration from three-dimensional to two-dimensional but changing the integration domain from the first Brillouin zone to the "energy-conservation" surface in the first Brillouin zone. The shape and location of this energy-conservation surface are determined in following manner: for every k_x, k_y pair a scan of the of the quantity $\Delta\omega = \omega_0 \pm \omega_1 - \omega_2$ is performed along k_z direction. A change of sign in $\Delta\omega$ indicates that the energy-conservation surface has been crossed; the value of the integrand is then carefully approximated at the crossing point. For a more precise determination of the position of the energy surface, additional gridding along the k_z direction is added. This additional gridding does not have the effect of increasing the density of the k-point mesh but only more precisely determining the location of the energy-conservation surface. Using these additional points helps resolve convergence issues, as described in the next chapter.

III. COMPUTATIONAL SETUP AND VALIDATION OF THE METHODS

In this section we validate our implementation of the calculation of thermal conductivity from BTE, using solid argon as a well-studied prototype. The solid phase of Ar has an fcc lattice with the cubic unit cell consisting of four atoms. The interatomic interactions are described by a standard Lennard-Jones (LJ) potential

$$V = 4\varepsilon \left[\left(\frac{r_0}{r} \right)^{12} - \left(\frac{r_0}{r} \right)^6 \right]. \tag{11}$$

There are a number of different parameterizations of the LJ potentials for argon. In order to make a direct comparison with previous work, we employ two different potentials. One parameterization, which we denote Potential I, is from the work of Omini and Sparavigna,[9] and has $\varepsilon = 0.009105$ eV, $r_0 = 3.445$ Å; the interaction cutoff is $2.5a_0$, where $a_0 = 5.326$ Å is the equilibrium lattice constant. The cutoff is implemented with a shifted-force function to ensure the continuity of energy and forces at the cutoff. We compare results of our implementation of the iterative procedure with previous work[9] using this potential. A second parameterization, which we denote Potential II, is from Turney *et al.* and has $\varepsilon = 0.01042$ eV and $r_0 = 3.40$ Å; the shifted-force interaction cutoff is $2.0a_0$, where $a_0 = 5.25$ Å. For this potential the values of the thermal conductivity have been determined from MD simulations.[13] Also, relaxation–time-approximation re-

TABLE I. Comparison of this implementation and literature values for thermal conductivity of solid argon using Omini and Sparavigna potential (Potential I). The lattice parameters are taken from experiment.

T (K)	$\Delta a/a_0$	k iterative (Ref. 9) (W/mK)	k iterative (this work) (W/mK)
20	0.001279	1.66	1.67
30	0.003600	1.00	1.03
40	0.006884	0.72	0.73
50	0.010791	0.58	0.54
60	0.015352	0.41	0.40
70	0.020672	0.31	0.30
80	0.027010	0.24	0.22

sults are available for Potential II. We, therefore, use this parameterization for comparison between different lattice dynamics methods, as well as for comparison with the MD simulations.

Lattice dynamics calculations are traditionally supposed to be performed at the zero-temperature equilibrium lattice constant; however the results at temperatures above $\sim T_m/3$, where T_m is the melting temperature are not accurate for any calculations based on the finite order perturbation theory, as was shown by Horton and Cowley.[17] The quasiharmonic approximation is the standard vehicle to overcome this difficulty, by treating force constants as dependent on the volume of the unit cell. The thermal conductivity of argon is very sensitive to the lattice constant;[12] hence for comparison with the previous work, identical simulation conditions must be used: when Potential I is employed we use lattice constants appropriate for a given temperature as obtained from experiment;[18] when Potential II is employed we use lattice constants determined by MD simulation with the same potential.[13] We note that these Lennard-Jones potentials overestimate thermal expansion of the argon.

We report results of the calculations for Potential I in Table I. All these calculations used a k-point grid of $9\times9\times9$ with additional gridding along the z axis of ten k points (see Appendix C). We note that the results of this implementation of the iterative procedure (column 4) are in excellent agreement with the previously reported data using this method (column 3). This agreement provides strong verification not only for the iterative method but also for the implementations of the relaxation-time approximation and variational methods since all three methods share the same subroutines for the computation of the scattering amplitudes, the most complicated part of the calculation.

Given that we have thus established the correctness of the implementation, we now address the saturation of the results with regards to the k-point grid and convergence with regards to number of iteration steps. The thermal conductivity for Potential I at $T=20$ K is used to investigate these issues.

Determination of the density of k points required to give converged results has two aspects. First, for a given $N\times N\times N$ grid, saturation of the result with additional refining k points along the z direction needs to be established. Second, saturation needs to be established as a function of N in the $N\times N\times N$ grid itself. The left panel in Fig. 1 shows the dependence of the thermal conductivity on the number of points in the refinement for the $9\times9\times9$ and $13\times13\times13$ integration grids. In both cases after ten additional points the result is converged to within 2% of the fully converged value. The right panel in Fig. 1 illustrates the necessity of this refinement. The open squares show the inverse thermal conductivity, $1/k$, as a function of $1/N$, but without additional refinement. This result demonstrates a linear trend, similar to that observed by Turney *et al.*[4] Such a linear trend was attributed to the inclusion of phonons of increasing wavelengths into the calculations with a denser k grid. However, the data with the additional refinement in the z direction shows that this is a result of a poor description of the energy conservation surface. Of course, a finer grid in all three k-space directions would provide a more accurate determination of the energy surface, as well as better sampling of the Brillouin zone, but is not practical because of the high computational load. Hence we use additional k points along the lines parallel to z axis as described above. Use of the grid with the additional refinement along z axis yields the data denoted by the solid circles in the right panel of Fig. 1. These results saturate to within 5% of the converged values for an

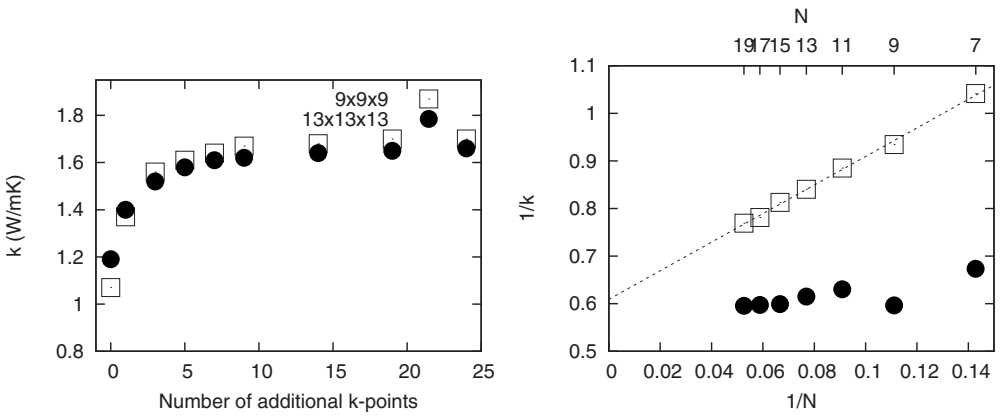

FIG. 1. Thermal conductivity as a function of the integration mesh parameters. Left panel: saturation of the result with the additional gridding. Right panel: saturation with the integration grid with (□) and without (●) refinement.

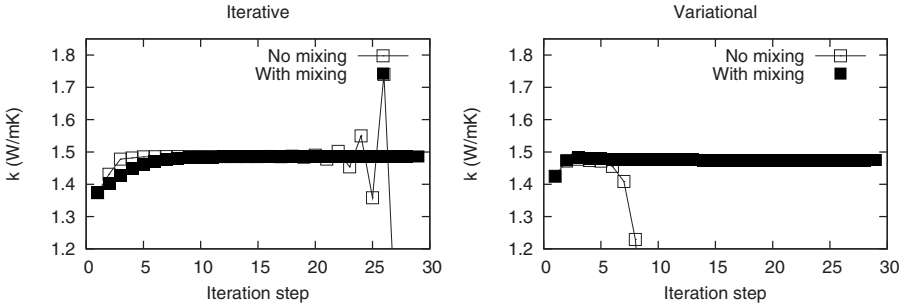

FIG. 2. Convergence of the iterative solution for $7\times7\times7$ k mesh at 20 K. Left panel shows the values of thermal conductivity as computed from Eq. (6) with and without mixing. Right panel shows thermal conductivity computed by variational formula [Eq. (7)], using perturbation from the iterative process. Notice, that with mixing it converges in 3–4 steps, compare to 10–12 step in iteration formula.

$11\times11\times11$ k mesh. By contrast, without refinement the thermal conductivity estimated with an $11\times11\times11$ k grid is only 60% of the converged value. Calculations on a wide variety of systems show that the underestimate of the thermal conductivity without z-axis refinement of the k mesh is endemic.[19]

We turn now to the number of iteration steps used in the iterative method. As discussed in Appendix A, the iterative technique is mathematically equivalent to the steepest descent algorithm for the solution of the system of linear equations. As such, the procedure is inherently convergent since the matrix of coefficients of these linear equations is positive definite and symmetric. Previous work however,[9] found that coarse k-mesh solutions might become unstable, an effect that we also observe. We attribute this behavior to deviations from the symmetry of the matrix caused by numeric errors associated with the accounting of the different types of the phonon processes. We find that by treating the iterative process as a self-consistency problem and applying very simple mixing rule, this problem can be eliminated

$$\vec{F}^{i+1}_{\vec{k},n} = \frac{1}{2}\vec{F}^{i}_{\vec{k},n} + \frac{1}{2}\left\{ \vec{F}^{0}_{\vec{k},n} + \frac{1}{Q_{\vec{k},n}} \int\int \sum_{n'n''} \left[(\vec{F}^{i}_{\vec{k}'',n''} - \vec{F}^{i}_{\vec{k}',n'})\Lambda^{\vec{k}'',n''}_{\vec{k},n;\vec{k}',n'} + \frac{1}{2}(\vec{F}^{i}_{\vec{k}',n'} + \vec{F}^{i}_{\vec{k}'',n''})\Lambda^{\vec{k}',n';\vec{k}'',n''}_{\vec{k},n} \right] d\vec{k}'\, d\vec{k}'' \right\}. \tag{12}$$

Examples of the convergence of the solution for the $7\times7\times7$ k meshes at 20 K are presented in Fig. 2. The left panel shows the thermal conductivity as a function of the number of iteration steps with and without mixing. Clearly, mixing completely eliminates oscillations in the result. For comparison, we also present in the right panel of the Fig. 2, the thermal conductivity as calculated by the variational formula [Eq. (7)] with the $\vec{F}^{i}_{\vec{k},n}$ as a variational function. We first note that without mixing, the solution shows a sharp decline in the thermal-conductivity value (indicating a strong decrease in the quality of the variational function) after the sixth step in the iteration process. It also indicates that the variational formula is significantly more sensitive to the numerical instability than Eq. (6). In contrast, mixed $\vec{F}^{i}_{\vec{k},n}$ produces a stable solution. Interestingly, the thermal conductivity computed from Eq. (7) converges to the final value in just 3–4 steps, comparing to 10–15 steps required by the iterative formula [Eq. (6)].

IV. COMPARISON OF LATTICE DYNAMIC METHODS

The results presented in this paper are all obtained by lattice dynamics methods and include only the three-phonon processes. To assess the appropriateness of this underlying assumption, it is necessary to have fiducial data (correct results) against which to compare these data. For a given potential we take the results obtained from molecular-dynamics simulations: either nonequilibrium molecular dynamics or Green-Kubo techniques. If the simulation temperature is high enough that the difference between quantum and classical phonon occupation numbers are not important, these classical methods should yield correct results. Although solid argon is not in the classical regime below ~50–60 K, it has been demonstrated[4] that 20 K is a sufficiently high temperature. However, it is important to remember that there are subtleties in the use of these methods also.[1] Moreover, these simulation techniques, while formally correct at high temperature, typically have fairly large error bars associated with them (10–15 % error is reported in Ref. 12 for Green-Kubo MD) and are very sensitive to such simulation details as the interaction cutoff. For example, different Green-Kubo MD simulations of the thermal conductivity of argon at 20 K, all using the same potential, but different cutoffs, and hence slightly different volumes, have yielded values of 0.90,[14] 1.1,[12] 1.2,[4] 1.57,[13] and 1.63 (Ref. 15) W/mK. At the same time, direct MD result from Turney *et al.*[4] yielded 1.4 W/mK. With such scattered data, it is not obvious what

TABLE II. Thermal conductivity of solid argon by Turney *et al.* potential.

T (K)	$\Delta a/a_0$	k GK-MD (Ref. 13) (W/mK)	k iterative (W/mK)	k variational (function from iterative) (W/mK)	k variational [functions set from Eq. (12)] (W/mK)	k relaxation time (W/mK)	k relaxation time (Ref. 4) (W/mK)
20	0.00939	1.57	1.66	1.66	1.50	1.48	1.50
30	0.01384	0.90	0.87	0.87	0.81	0.79	0.93
40	0.01868	0.57	0.60	0.60	0.53	0.53	0.66
50	0.02408	0.42	0.43	0.43	0.39	0.38	0.51
60	0.03028	0.33	0.31	0.31	0.27	0.27	0.40
70	0.03733	0.24	0.26	0.26	0.22	0.23	0.32
80	0.04602	0.22	0.19	0.19	0.16	0.17	0.27

is the best fiducial data to use. Our choice is to reproduce the conditions for the calculations reported in Ref. 13 exactly: all parameters for Potential II (cutoff, energy, and length scale) and unit-cell volumes are taken from there.

Table II presents the results of simulations of the thermal conductivity by the Green-Kubo method[13] (column 3), and the values obtained in this work with the iterative method (column 4), variational method (column 5—with perturbation function obtained by iterative method, and column 6 with generic perturbation functions, see below), and the relaxation time approximation (Column 7). Column 8 contains the results of previous calculations using the relaxation time approximation by Turney *et al.*

First, comparing the full iterative solution to Green-Kubo molecular-dynamics results,[13] we see good overall agreement. While the two methods yield somewhat different values, there is no systematic deviation: some are larger in MD, others are larger in lattice dynamics. We ascribe these differences to numerical errors. Since the MD simulations also include processes of more than three phonons, we conclude that in the case of solid argon, three-phonon processes are sufficient to represent the thermal-transport properties. Omini and Sparavigna[9] reached the same conclusion on the basis of the agreement with the experimental data for solid argon while Turney *et al.* reached the opposite conclusion based on the relaxation time approximation results; we discuss this issue further below.

Second, the variational technique provides essentially the same results as iterative method if a converged $\vec{F}^i_{\vec{k},n}$ is used as a trial function. This is expected, since Eqs. (6) and (7) are equivalent, when $\vec{F}^i_{\vec{k},n}$ is the solution of the BTE. Actually, we observed that even a nonfully converged $\vec{F}^i_{\vec{k},n}$ is a very good choice of trial function since even the first iteration produces an estimate of the thermal conductivity within 10% of the converged value (see Fig. 2).

We have assessed the capabilities of ten "standard" choices for the trial functions;[8] these include trial functions based on the k vector, the group velocity, and their products with various powers of the phonon frequency

$$\vec{F}_{\vec{k},n} = \vec{k} \cdot \omega^i_{\vec{k},n}, \quad i = -2,-1,0,1,2,$$

$$\vec{F}_{\vec{k},n} = \vec{v}_{\vec{k},n} \cdot \omega^j_{\vec{k},n}, \quad j = -2,-1,0,1,2. \tag{13}$$

The first of these functions is motivated by the fact that it produces correct, infinite thermal conductivity if only normal processes are taken into account. However, it has the shortcoming that there are always modes that produce heat flow along the thermal gradient direction, thereby reducing the calculated thermal conductivity. The group-velocity trial function is an attempt to correct that issue since it guarantees that each mode transfers heat against temperature gradient.

None of these functions individually produces converged values of thermal conductivity closer than 75% of the iterative result. The standard choice of the k vector as a trial function turns out to be a poor choice, the thermal conductivity being two orders of magnitude smaller than the full solution, indicating the (well-known) importance of the Umklapp processes. Of the standard variational functions, the best function is the group velocity of the phonons: $\vec{F}_{\vec{k},n} = \vec{v}_{\vec{k},n}$; this typically generates value of thermal conductivity of about 75% of the iterative result.

Given that none of the variational functions matches the correct results alone, it is interesting to explore the effects of linear combination. A linear combination of functions in Eq. (13) when optimized can typically produce values for the thermal conductivity in excess of 90% of the full solution, as indicated in column 6 of Table II. In principle, of course, one is not limited to these 10 functions at all. One can use any set of "basis" functions in the three-dimensional k space to describe the trial function. We built such a basis from the Chebyshev polynomials (assuming temperature gradient is in z direction)

$$F^z_{\vec{k},n} = T_p(v^x_{\vec{k},n}/v^x_{\max}) T_q(v^y_{\vec{k},n}/v^y_{\max}) T_l(v^z_{\vec{k},n}/v^z_{\max}),$$

$$l = 1,3,5,7,9, \quad p,q = 0,2,4,6,8. \tag{14}$$

The specific appropriate choice of p, q, and l values is related to the symmetry properties of the perturbation function: it has to be odd along the temperature gradient direction and

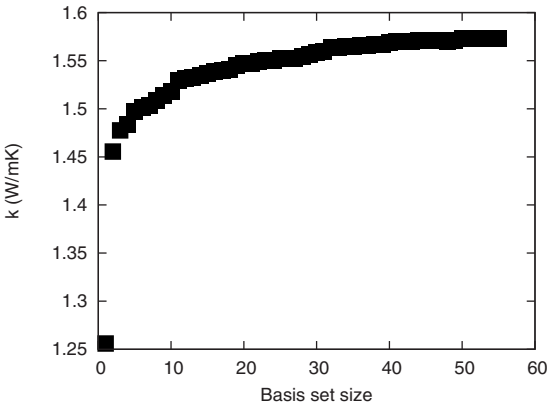

FIG. 3. Thermal conductivity by variational method as a function of the size of the basis set.

even in any direction perpendicular to it. The choice of Chebyshev polynomials is dictated by their numerical convenience and their excellent convergence properties (group velocities are normalized to maximum value in order to ensure argument range of $[-1,1]$, the interval of interest for Chebyshev polynomials). Figure 3 presents the thermal conductivity at 20 K as predicted by the variational method versus the number of basis functions in Eq. (14) used in the expansion. The calculated thermal conductivity converges slowly; for the largest number of basis functions we looked at, 55, the result is 1.57 W/mK, about 95% of the true value. Hence the variational method can be a viable alternative to other methods. Its applicability to other systems requires additional investigation.

Third, the relaxation time approximation (column 7) slightly underestimates the thermal conductivity, a result also reported previously for argon and other systems.[9,10] However, this behavior is not universal, and we have observed that in some other materials, the relaxation-time approximation produces results virtually identical with the full solution;[19] we have also found materials for which the relaxation-time approximation overestimates the correct value.[19] This is a direct consequence of the relaxation-time approximation being an intrinsically uncontrolled approximation: in contrast to the variational method the direction of the error is undetermined.

Comparing our results using the relaxation-time approximation with previously published data,[4] we observe that our implementation consistently produces lower values of the thermal conductivity, especially at high temperature. We attribute this to two factors. First, we use a different method for treating the δ function describing the conservation of energy in the three-phonons processes. Turney *et al.* used a Lorentzian representation with variable width, the latter being controlled by the half-width of the phonons states Γ_λ

$$\delta(\omega_\lambda + \omega_{\lambda'} - \omega_{\lambda''}) = \frac{1}{\pi}\frac{\varepsilon}{(\omega_\lambda + \omega_{\lambda'} - \omega_{\lambda''})^2 + \varepsilon^2},$$
$$\varepsilon = \Gamma_\lambda + \Gamma_{\lambda'} + \Gamma_{\lambda''}. \quad (15)$$

As the temperature increases, this broadening increases as well, resulting in a wider and lower peak for the δ function representation; a self-consistent procedure is used for the phonon states half-width Γ_λ Ideally, the result of the numerical integration over the representation of the δ function in Eq. (15) should not depend on the broadening parameter: a wider peak will add a contribution from the neighboring integration points, offsetting the lowering of the peak. However if the relatively coarse k-point mesh is used for the integration (we found that even $20\times20\times20$ is still too coarse) then these neighboring points are too far away to make a contribution. As a result this method can lead to an underestimate of equilibrium transition rates and phonon half-widths, resulting in an overestimate in the thermal conductivity, especially at high temperature. To avoid this effect, our calculations do not use an approximation for the δ function but integrate explicitly over the "energy conservation" surface (see above and Appendix C for a complete description). Second, only nearest neighbors are taken into account for the anharmonic calculations in Turney *et al.*, an assumption that usually leads to an overestimate of the thermal conductivity in lattice dynamics[9] (Also, different equilibrium volumes were used in Ref. 4) Our results therefore, do not support the notion that lattice dynamics methods intrinsically overestimate the thermal conductivity at high temperature, as was suggested by Turney *et al.*, at least for solid argon.

Comparing the various methods, we observe that the iterative method produces reliable and consistent results. The variational method and relaxation-time approximation generally produces thermal conductivity within 25% of the true value. The advantage of the variational method relative to the relaxation-time approximation is the fact that it is guaranteed to produce a lower bound for the three-phonon contribution to thermal conductivity while the relaxation time approximation can have an error in either direction. A disadvantage of the variational method is that a single set of calculations produces only one component of the thermal conductivity tensor.

Concluding the comparison of the different methods for calculating thermal conductivity, we address the issue of the computational load. We recall that the integration of the k vectors over the Brillouin zone [see Eq. (5)] is the bottleneck in the calculations. The relaxation-time approximation and the variational method with "generic" trial functions require only one double integration over the Brillouin zone. However, these result in errors in the thermal conductivity of 25% and 10%, respectively. The variational method with $\vec{F}^i_{\vec{k},n}$ as a trial function requires at least two iterations (i.e., takes approximately twice as long), for which the error is reduced to about 10%; 3–4 iterations produces full convergence. The iterative method requires 10–15 steps for achieving convergence. Thus from a computational point of view, the iterative procedure with a variational formula for thermal conductivity produces the highest fidelity results with the fewest number of calculations.

Solution of the BTE by these methods also allows the calculation of a number of other characteristics of the system, including individual phonon relaxation times, and contributions to the thermal conductivity as a function of phonon

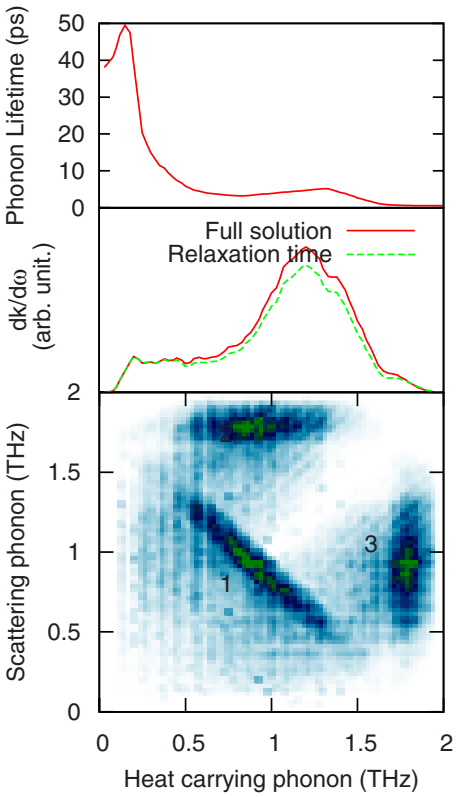

FIG. 4. (Color online) Top panel: averaged phonon lifetimes as a function of frequency. Middle panel: contribution to the thermal conductivity from the phonons with a given frequency (solid line—full solution, dashed line—relaxation-time approximation). Bottom panel: map of the cumulative scattering amplitude.

energy or momentum. Detailed insights into phonon-phonon scattering can also be obtained, as illustrated in Fig. 4; all the data is for temperature of 20 K. The top panel shows average phonon lifetimes; the middle panel shows the contribution to the thermal conductivity from the phonons of each frequency. These spectral contributions are presented from the relaxation-time approximation (dashed curve) and the full iterative solution (solid curve). This shows that the larger values of the thermal conductivity by the iterative method compared to the relaxation-time approximation are produced by the increased contributions from the phonons with frequencies in the 0.5–1.5 THz range. Comparison of the top and middle panel also demonstrates that while low-energy phonons (below 0.2 THz) are the longest living phonons, they produce relatively small contribution to the thermal conductivity due to the limited number of available states and small amount of energy that they can carry. The bottom panel of Fig. 4 shows a map of the scattering amplitudes for phonons: the darker the color, the larger the cumulative amplitude of the processes that involves phonons with the frequencies on the horizontal and vertical axes. This combined map shows processes with both $\omega_0+\omega_1=\omega_2$ and $\omega_0=\omega_1+\omega_2$, with ω_0 along the horizontal axis and ω_1 and ω_2 along the vertical axis. This map has three distinct areas. Areas 1 and 2 represent the amplitude of the process of two phonons scattering to one. Area 3 contains the process of one phonon scattering into two phonons. Clearly, the dominant process (the brightest spots on the map) involves phonons with high frequency (1.6–1.8 THz) splitting into two phonons, with the lower frequency 0.8–0.9 THz, and the reverse process. This strong scattering of the high-frequency phonons creates an excess of phonons in the midfrequency range (0.5–1.5 THz); that is, their distribution most strongly deviates from the equilibrium, making them the major heat carriers. Due to the large number of three-phonon processes they can participate in, the distribution of high-frequency phonons rapidly returns to the equilibrium value. Therefore, they do not make a significant contribution to the thermal conductivity.

V. CONCLUSIONS

In conclusion, we have presented a direct comparison of three different methods for computing the thermal conductivity from the solution of the Boltzmann transport equation. All the necessary mathematical apparatus has been presented, as well as technical details of the implementation. The iterative method predicts thermal conductivity in close agreement with MD data while the variational method and relaxation time approximation underestimate it by ~10% and ~25% correspondingly. The other findings of this paper are the following: (a) additional gridding for more precise determination of the integration surface is a reliable and consistent method to ensure rapid convergence of the computed value of thermal conductivity with respect to k-point mesh. (b) The iterative method is inherently convergent, as has been observed in practice. (c) A simple mixing rule is a reliable way to achieve stability of the iterative process even for the coarse k-point grids. (d) The combination of the iterative technique for computing consecutive approximations to the solution to the BTE [Eq. (2)] and variational formula [Eq. (7)] to compute thermal conductivity from these approximations is the fastest way to reach convergent values for the thermal conductivity on the example of the solid argon. (e) These methods allow the connections between thermal conductivity and phonon properties to be determined.

Finally, this paper demonstrates that at least in simple solids, cubic term in the energy expansion suffice to determine thermal conductivity over a wide temperature range. This might not be the case for ionic materials that have a large variety of complicated atomic structures. Additional difficulty in the ionic materials is a long-range electrostatic interactions, influence of which requires additional investigations.

ACKNOWLEDGMENTS

We are grateful to Joe Turney and Alan McGaughey of Carnegie Mellon University for valuable discussions. This work was supported by DARPA, Materials World Network Project, NSF under Grant No. DMR-0710523 and the DOE-BES Computational Materials Science Network Project on "Multiscale simulation of thermomechanical processes in irradiated fission-reactor materials."

APPENDIX A: BTE AND SOLUTION METHODS

1. Linearized Boltzmann equation

Although long established (see, for example Refs. 3 and 5), it is useful to rehearse the analysis of the linear BTE as it

helps establish the nomenclature to be used throughout these appendices. The probability density distribution function, $f_\lambda(\vec{r})$, describes the probability of finding a particle in some state labeled by λ in the region around point $\vec{r}$ in space. The value of $f_\lambda(\vec{r})$ can change for a number of reasons: (i) if the distribution function has a nonzero gradient, then the number of particles in the region will change with a rate proportional to the gradient and to the velocity $\vec{v}$ of the particles (diffusive, or entropic term); (ii) if there are external forces acting on the system, the particles will move; and (iii) particles may interact with each other (variously called the interaction term, the scattering term or the collision integral). In equilibrium (or under steady-state conditions) the value of the distribution function should be constant at any point; hence the rate of change in the probability distribution arising from all three terms must be zero

$$\dot{f}_\lambda(\vec{r}) = \dot{f}_\lambda(\vec{r})_{diff} + \dot{f}_\lambda(\vec{r})_{ext} + \dot{f}_\lambda(\vec{r})_{scatt} = 0. \tag{A1}$$

The diffusive term can be understood in the frame of reference that moves with the particle. If at time zero it was $f_\lambda(\vec{r})$, it becomes $f_\lambda(\vec{r}+\vec{v}t)$ at a later time t due to particle motion

$$\dot{f}_\lambda(\vec{r})_{diff} = -\vec{v}_\lambda \cdot \frac{\partial f_\lambda(\vec{r})}{\partial \vec{r}}. \tag{A2}$$

The external force term, $\dot{f}_\lambda(\vec{r})_{ext}$, depends on the type of particles considered. For example, electrons can be subject to a force arising from an electric or magnetic field. As we are interested in phonons, this external force term can be taken to be zero. Finally, the scattering term describes the effect of interaction either among particles or between particles and imperfections in the lattice. This term has the effect of changing the state of the particle. We split this term into probabilities, P, from events when a single phonon change its state, $P_{\lambda\lambda'}$, such as scattering from lattice defects; three phonon process, $P_{\lambda\lambda'\lambda''}$ and high order terms such as electron-electron collisions and fourth-order in phonon-phonon interactions, $P_{\lambda\lambda'\lambda''\lambda'''}$

$$-\dot{f}_\lambda(\vec{r})_{scatt} = \sum_{\lambda'} P_{\lambda\lambda'} + \sum_{\lambda'\lambda''} P_{\lambda\lambda'\lambda''} + \sum_{\lambda'\lambda''\lambda'''} P_{\lambda\lambda'\lambda''\lambda'''} + \cdots. \tag{A3}$$

The net probability for each individual process is the difference between processes in which particles leaves state λ and the inverse processes in which particles enter state λ; hence for the first term in the Eq. (A3) we have

$$P_{\lambda\lambda'} = f_\lambda(1 \pm f_{\lambda'})L_\lambda^{\lambda'} - (1 \pm f_\lambda)f_{\lambda'}L_{\lambda'}^{\lambda}. \tag{A4}$$

In this expression we also separate the occupation numbers of the initial and final state. The quantity L is called the intrinsic probability of the transition. The plus (minus) signs in the brackets correspond to the case of bosons (fermions). For fermions, transitions are prohibited if there are no particles in the initial state, or if the final state is occupied, reflecting the Pauli principle. For bosons there is no restriction on the number of particles in the final state. In fact, the transition probability is enhanced if there is particle present in the final state: this is known as a stimulated emission phenomenon. Mathematically, this stimulated emission comes from the normalization conditions for the matrix element of the creation and annihilation operators in the case of bosons, as will be illustrated below.

In a similar manner, the three-particle probability can be written as

$$\begin{aligned} P_{\lambda\lambda'\lambda''} = {} & f_\lambda f_{\lambda'}(1 \pm f_{\lambda''})L_{\lambda\lambda'}^{\lambda''} - (1 \pm f_\lambda)(1 \pm f_{\lambda'})f_{\lambda''}L_{\lambda''}^{\lambda\lambda'} \\ & + \frac{1}{2}[f_\lambda(1 \pm f_{\lambda'})(1 \pm f_{\lambda''})L_\lambda^{\lambda'\lambda''} \\ & - (1 \pm f_\lambda)f_{\lambda'}f_{\lambda''}L_{\lambda'\lambda''}^{\lambda}]. \end{aligned} \tag{A5}$$

The factor of one-half in front of final two terms is for when a particle in state λ is produced as a result of interaction of two particles in states λ' and λ'', for which interchange of λ' and λ'' represents the same process. Corresponding expressions can be written for the four particles processes.

A phonon in an infinite, periodic solid is described by two variables: the reciprocal lattice vector, $\vec{k}$, and a phonon-branch index n. As a result, summations over all the states in the above equations involve integration over the Brillouin zone and summation over the branch index. Thus the BTE is a nonlinear integrodifferential equation that is essentially impossible to solve analytically. The first simplification step is to linearize the BTE using the following ansatz:

$$f_\lambda = f_\lambda^0 - \Phi_\lambda \frac{\partial f_\lambda^0}{\partial E_\lambda}, \tag{A6}$$

where f_λ^0 is the equilibrium Bose-Einstein distribution function hence the derivative is easily calculated. E_λ is the energy of the state λ, and Φ_λ is the perturbation in the distribution function, which is assumed small. One further assumes that local equilibrium is maintained at each point in space, $\vec{r}$, but that the temperature might change from point to point. This implies that Φ_λ depends on position $\vec{r}$ only through temperature. As a result, the diffusive term can be written as

$$-\vec{v}_\lambda \cdot \frac{\partial f_\lambda(\vec{r})}{\partial \vec{r}} \approx -\vec{v}_\lambda \cdot \frac{\partial f_\lambda^0}{\partial T} \nabla T. \tag{A7}$$

Substituting the ansatz from Eq. (A6), into the expression for the probability P, and keeping terms to first order in Φ_λ we obtain

$$P_{\lambda\lambda'} = \frac{1}{kT}(\Phi_\lambda - \Phi_{\lambda'})f_\lambda^0(1 \pm f_{\lambda'}^0)L_n^{n'} = \frac{1}{k_B T}(\Phi_\lambda - \Phi_{\lambda'})\Lambda_\lambda^{\lambda'}, \tag{A8}$$

where we used the fact that by the principle of the detailed balance $L_\lambda^{\lambda'} = L_{\lambda'}^{\lambda}$. The $1/k_bT$ prefactor arises from the derivative of the equilibrium distribution function. A similar expression can be derived for the three-particle term

$$P_{\lambda\lambda'\lambda''} = \frac{1}{k_B T}\{(\Phi_\lambda + \Phi_{\lambda'} - \Phi_{\lambda''}) f^0_\lambda f^0_{\lambda'}(1 \pm f^0_{\lambda''}) L^{\lambda''}_{\lambda\lambda'}\} + \frac{1}{k_B T}\left\{\frac{1}{2}(\Phi_\lambda - \Phi_{\lambda'} - \Phi_{\lambda''}) f^0_\lambda (1 \pm f^0_{\lambda'})(1 \pm f^0_{\lambda''}) L^{\lambda'\lambda''}_{\lambda}\right\}$$
$$= \frac{1}{k_B T}\left\{(\Phi_\lambda + \Phi_{\lambda'} - \Phi_{\lambda''})\Lambda^{\lambda''}_{\lambda\lambda'} + \frac{1}{2}(\Phi_\lambda - \Phi_{\lambda'} - \Phi_{\lambda''})\Lambda^{\lambda'\lambda''}_{\lambda}\right\} \tag{A9}$$

Λ is the equilibrium transition rate between the states defined by its subscripts and superscripts, defined as the number of transitions per unit of time if the system is in thermodynamic equilibrium. In all these expressions we also use the fact that in thermodynamic equilibrium ($f_\lambda = f^0_\lambda$) the scattering term vanishes. Higher order terms are similar. Collecting all these together, we obtain the following linearized BTE (sometimes also called canonical form of BTE)

$$-\vec{v}_\lambda \cdot \frac{\partial f^0_\lambda}{\partial T} \nabla T = \frac{1}{k_B T}\left\{\sum_{\lambda'} (\Phi_\lambda - \Phi_{\lambda'})\Lambda^{\lambda'}_{\lambda} + \sum_{\lambda'\lambda''}\left[(\Phi_\lambda + \Phi_{\lambda'} - \Phi_{\lambda''})\Lambda^{\lambda''}_{\lambda\lambda'} + \frac{1}{2}(\Phi_\lambda - \Phi_{\lambda'} - \Phi_{\lambda''})\Lambda^{\lambda'\lambda''}_{\lambda}\right] + \cdots\right\}. \tag{A10}$$

This equation is fairly general and applicable to either electrons or phonons in the solids (by selecting appropriate processes that is possible for the particular particles). All the details of the interactions among particles are encapsulated in the parameters Λ; the exact form of these parameters does not affect the solution methods that we discuss in the next session.

2. Solution methods

There are a variety of solution methods for analyzing the BTE. In particular, in the case of electrons (electrical conductivity is a transport property) there is a vast literature[20] that discusses methods ranging from Monte Carlo methods to linear algebra and path integral techniques. Application of these methods is possible due to the fact that usually only two-particles events need be taken into account: three electron events are impossible and four electron events are very rare. As a result, only a single integration over the Brillouin zone is required. For the case of phonons, three-particle interactions are present and are the dominant contribution to the intrinsic thermal conductivity of materials. In this section we discuss in details three methods for analyzing the BTE with three-phonon processes and determining the thermal conductivity: an iterative approach,[9] a variational method,[5] and a relaxation-time approximation.[4]

3. Iterative solution

From the conceptual perspective, the iterative approach is (deceptively) simple. Let us start by writing the BTE for three-phonon processes only, where from Eq. (A10), we have calculated the derivative on the left-hand side

$$-\frac{E_\lambda}{k_B T^2} f^0_\lambda (1 + f^0_\lambda)\vec{v}_\lambda \cdot \nabla T = \frac{1}{k_B T}\left\{\sum_{\lambda'\lambda''}\left[(\Phi_\lambda + \Phi_{\lambda'} - \Phi_{\lambda''})\Lambda^{\lambda''}_{\lambda\lambda'} + \frac{1}{2}(\Phi_\lambda - \Phi_{\lambda'} - \Phi_{\lambda''})\Lambda^{\lambda'\lambda''}_{\lambda}\right]\right\}. \tag{A11}$$

We proceed by representing the perturbation to the distribution function as

$$\Phi_\lambda = \vec{F}_\lambda \cdot \nabla T. \tag{A12}$$

Substituting into Eq. (A11), we obtain

$$\left\{f^0_\lambda (1 + f^0_\lambda) E_\lambda \vec{v}_\lambda - T\sum_{\lambda'\lambda''}\left[(\vec{F}_\lambda + \vec{F}_{\lambda'} - \vec{F}_{\lambda''})\Lambda^{\lambda''}_{\lambda\lambda'} + \frac{1}{2}(\vec{F}_\lambda - \vec{F}_{\lambda'} - \vec{F}_{\lambda''})\Lambda^{\lambda'\lambda''}_{\lambda}\right]\right\} \cdot \nabla T = 0. \tag{A13}$$

Equating the contents of the curly brackets to zero and pulling $\vec{F}_\lambda$ from under summation sign we get

$$f^0_\lambda (1 + f^0_\lambda)\vec{v}_\lambda E_\lambda - T\sum_{\lambda'\lambda''}\left[(\vec{F}_{\lambda'} - \vec{F}_{\lambda''})\Lambda^{\lambda''}_{\lambda\lambda'} + \frac{1}{2}(-\vec{F}_{\lambda'} - \vec{F}_{\lambda''})\Lambda^{\lambda'\lambda''}_{\lambda}\right] = T\vec{F}_\lambda \sum_{\lambda'\lambda''}\left[\Lambda^{\lambda''}_{\lambda\lambda'} + \frac{1}{2}\Lambda^{\lambda'\lambda''}_{\lambda}\right]. \tag{A14}$$

Introducing the new variable

$$Q_\lambda = \sum_{\lambda'\lambda''}\left[\Lambda^{\lambda''}_{\lambda\lambda'} + \frac{1}{2}\Lambda^{\lambda'\lambda''}_{\lambda}\right] \tag{A15}$$

and rearranging the terms yields the self-consistency equation

$$\vec{F}_\lambda = -\frac{f_\lambda^0(1+f_\lambda^0)\vec{v}_\lambda E_\lambda}{TQ_\lambda} + \frac{1}{Q_\lambda}\sum_{\lambda'\lambda''}\left[(\vec{F}_{\lambda''}-\vec{F}_{\lambda'})\Lambda_{\lambda\lambda'}^{\lambda''} + \frac{1}{2}(\vec{F}_{\lambda'}+\vec{F}_{\lambda''})\Lambda_{\lambda}^{\lambda'\lambda''}\right]. \tag{A16}$$

Numerical solutions to this equation can be found by iteration

$$\vec{F}_\lambda^{i+1} = \vec{F}_\lambda^0 + \frac{1}{Q_\lambda}\sum_{\lambda'\lambda''}\left[(\vec{F}_{\lambda''}^i-\vec{F}_{\lambda'}^i)\Lambda_{\lambda\lambda'}^{\lambda''} + \frac{1}{2}(\vec{F}_{\lambda'}^i+\vec{F}_{\lambda''}^i)\Lambda_{\lambda}^{\lambda'\lambda''}\right], \quad i=1,2,3,\ldots. \tag{A17}$$

With the initial condition

$$\vec{F}_\lambda^0 = -\frac{f_\lambda^0(1+f_\lambda^0)\vec{v}_\lambda E_\lambda}{TQ_\lambda}, \quad \vec{F}_\lambda^1 = 0. \tag{A18}$$

Once $\vec{F}_\lambda^{i+1}=\vec{F}_\lambda^i$ within some tolerance for all λ, the solutions are self-consistent, and the iterative process is terminated.

The thermal conductivity may then be calculated by using Fourier's law $U_\alpha=-k_{\alpha\beta}\nabla_\beta T$ and an expression for the heat current $\vec{U}$ in terms of the distribution function

$$\vec{U} = \sum_\lambda E_\lambda \vec{v}_\lambda f_\lambda = \sum_\lambda E_\lambda \vec{v}_\lambda\left(f_\lambda^0 - \frac{\partial f_\lambda^0}{\partial E_\lambda}\Phi_\lambda\right)$$
$$= \sum_\lambda E_\lambda \vec{v}_\lambda \frac{f_\lambda^0(1+f_\lambda^0)}{k_B T}\vec{F}_\lambda\cdot\nabla T = \sum_\lambda E_\lambda \vec{v}_\lambda \frac{f_\lambda^0(1+f_\lambda^0)}{k_B T}\vec{F}_\lambda\cdot\nabla T, \tag{A19}$$

where the first term in the brackets disappears since there is no heat current in the thermal equilibrium. This produces the following expression for the thermal conductivity tensor:

$$\bar{k} = -\sum_\lambda E_\lambda \frac{f_\lambda^0(1+f_\lambda^0)}{k_B T}\vec{v}_\lambda \otimes \vec{F}_\lambda^i. \tag{A20}$$

The last issue to be addressed is the convergence of the procedure. Equation (A17) can be viewed as a set of linear equations

$$A_{\lambda\lambda'}F_{\lambda'} = b_\lambda,$$

$$A_{\lambda\lambda'} = \delta_{\lambda\lambda'} + \frac{1}{Q_\lambda}\sum_{\lambda''}\left(-\Lambda_{\lambda\lambda''}^{\lambda'} + \Lambda_{\lambda\lambda'}^{\lambda''} - \frac{1}{2}\Lambda_\lambda^{\lambda'\lambda''} - \frac{1}{2}\Lambda_{\lambda'}^{\lambda\lambda''}\right),$$

$$b_\lambda = -\frac{f_\lambda^0(1+f_\lambda^0)\vec{v}_\lambda E_\lambda}{TQ_\lambda}. \tag{A21}$$

Rewriting them in this way makes it clear that the iterative procedure is nothing but a simple implementation of the conjugate gradient method that is guaranteed to converge, if the matrix $A_{\lambda\lambda'}$ is symmetric and positive definite.[21] Using the properties of the equilibrium transitions rates, Λ, see Eq. (B11), one can easily show the symmetry; positive-definiteness is explicitly demonstrated in Eq. (B12) for the operator representing BTE. While, in principle, in the worst case scenario convergence requires a number of steps equal to the dimension of the matrix $A_{\lambda\lambda'}$, in practice satisfactory convergence for thermal conductivity occurs in as few as ten iterations. A nice feature of this approach is that one obtains complete thermal conductivity tensor from one set of calculations.

4. Variational solution

The linearized BTE in its canonical form, Eq. (A10), can be viewed as $X=P\Phi$, where P is a linear operator. This equation may be analyzed using variational methods if the operator P obeys appropriate conditions on symmetry and positive definiteness[5,22]

$$\langle\Psi,P\Phi\rangle = \langle\Phi,P\Psi\rangle,$$

$$\langle\Phi,P\Phi\rangle > 0, \quad \text{for any } \Phi, \tag{A22}$$

where $\langle\ldots\rangle$ represent the scalar product between two functions; the function Φ_λ is a function of the state λ, hence $\langle\Psi_\lambda,\Phi_\lambda\rangle=\Sigma_\lambda\Psi_\lambda\Phi_\lambda$. As we will see in the following, the P operator that represents phonons interactions obeys properties of Eq. (A22). Multiplying the BTE by Φ on both sides of the equation, we obtain

$$\langle\Phi,X\rangle = \langle\Phi,P\Phi\rangle. \tag{A23}$$

The variational principle then states that the function Φ, which is the exact solution to BTE, maximizes the value of $\langle\Phi,P\Phi\rangle$. This can be proven by considering another function Ψ, that satisfies $\langle\Psi,X\rangle=\langle\Psi,P\Psi\rangle$, but not a solution to BTE itself. Then

$$0 \le \langle(\Phi-\Psi),P(\Phi-\Psi)\rangle = \langle\Phi,P\Phi\rangle + \langle\Psi,P\Psi\rangle - 2\langle\Psi,P\Phi\rangle$$
$$= \langle\Phi,P\Phi\rangle + \langle\Psi,P\Psi\rangle - 2\langle\Psi,X\rangle = \langle\Phi,P\Phi\rangle + \langle\Psi,P\Psi\rangle$$
$$- 2\langle\Psi,P\Psi\rangle = \langle\Phi,P\Phi\rangle - \langle\Psi,P\Psi\rangle. \tag{A24}$$

In this derivation we have used positive definiteness and linearity of P and the fact that Φ obeys the BTE. A more convenient form of the variational principle for practical applications (including calculating the thermal conductivity) is

$$\frac{\langle\Phi,P\Phi\rangle}{\langle\Phi,X\rangle^2} = \min. \tag{A25}$$

In order to see why, consider the left-hand side of the BTE, multiplied by Φ

$$-\left\langle \Phi_\lambda, \vec{v}_\lambda \cdot \frac{\partial f_\lambda^0}{\partial T} \nabla T \right\rangle = \frac{\nabla T}{T} \cdot \sum_\lambda \Phi_\lambda \vec{v}_\lambda E_\lambda \frac{\partial f_\lambda^0}{\partial E_\lambda}$$

$$= -\frac{\vec{U}}{kT} \cdot \sum_\lambda \Phi_\lambda \vec{v}_\lambda E_\lambda \frac{\partial f_\lambda^0}{\partial E_\lambda}$$

$$= \frac{1}{kT}\left(\sum_\lambda \Phi_\lambda \vec{v}_\lambda E_\lambda \frac{\partial f_\lambda^0}{\partial E_\lambda} \right)^2$$

$$= \frac{T}{k}\left(\sum_\lambda \Phi_\lambda \vec{v}_\lambda \frac{\partial f_\lambda^0}{\partial T} \right)^2$$

$$= \frac{T}{k}\left(\sum_\lambda \Phi_\lambda \vec{v}_\lambda \frac{\partial f_\lambda^0}{\partial T} \right)^2 = \frac{T}{k} \langle \Phi, X \rangle^2 |_{\nabla T=1}, \tag{A26}$$

where we have again used the fact that heat current is zero in equilibrium. Collecting all the terms together, we see that inverse of thermal conductivity k reaches its minimum value, when Φ is the solution of the BTE (in the unity temperature gradient)

$$\frac{1}{k} = \frac{1}{T} \min \frac{\langle \Phi, P\Phi \rangle}{\langle \Phi, X \rangle^2 |_{\nabla T=1}}. \tag{A27}$$

From this point, the calculation of thermal conductivity proceeds in the standard manner for variational methods. Linear combination of known trial functions ϕ_i are chosen: $\Phi = \Sigma_i c_i \phi_i$; variational integrals $P_{ij}=(\phi_i, P\phi_j)$ and $X_i=(\phi_i, X)$ are evaluated. The set of coefficients c_i that minimizes the variational function yields the best approximation (for these trial functions) for the inverse of thermal conductivity. This set might be found by solving $P_{ij}c_j=X_i$. In order to see that this is equivalent to the minimum of the variation function we minimize it [Eq. (A27)] with respect to coefficient c_k and use $P_{ij}c_ic_j=X_ic_i$.

5. Relaxation-time approximation

Finally, let us discuss the relaxation time approximation. In this method, the scattering integral in the initial Boltzmann equation is approximated as

$$-\dot{f}_\lambda(\vec{r})_{scatt} = \frac{f_\lambda - f_\lambda^0}{\tau_\lambda} \tag{A28}$$

effectively absorbing all the interactions details for each mode into a single state-dependent relaxation time, τ_λ. From the perspective of many-body theory, a small perturbation to the Hamiltonian can be seen as producing two effects: shifting the eigenvalues of the unperturbed Hamiltonian and providing a finite lifetime to these states. The finite lifetime is usually described by the linewidth of a state in the presence of the perturbation. Detailed analysis of the many-body perturbation theory for phonons was performed by Maradudin and Fein,[16] who derived the following expression for the linewidth, also used by:[4]

$$\Gamma_\lambda = \frac{\pi\hbar}{16N} \sum_{\lambda'\lambda''} |\Gamma_{\lambda\lambda'\lambda''}|^2 \{ [f_{\lambda'}^0 + f_{\lambda''}^0 + 1][\delta(E_\lambda - E_{\lambda'} - E_{\lambda''})]$$

$$+ [f_{\lambda'}^0 - f_{\lambda''}^0][\delta(E_\lambda + E_{\lambda'} - E_{\lambda''}) - \delta(E_\lambda - E_{\lambda'} + E_{\lambda''})] \} \tag{A29}$$

here, $\Gamma_{\lambda\lambda'\lambda''}$ is a Fourier transform of the cubic term in the expansion of the total energy (see Appendix B). The relaxation time is then inversely proportional to the linewidth

$$\tau_\lambda = \frac{1}{2\Gamma_\lambda}. \tag{A30}$$

Using Eqs. (A1), (A7), and (A28), we obtain for the deviation of the distribution function

$$f_\lambda - f_\lambda^0 = \vec{v}_\lambda \cdot \frac{\partial f_\lambda^0}{\partial T} \nabla T \tau_\lambda. \tag{A31}$$

Substituting this into the expression for the heat current, Eq. (A19), and applying Fourier's law we obtain the expression for thermal conductivity tensor

$$\bar{k} = \sum_\lambda E_\lambda^2 \frac{f_\lambda^0 (1 + f_\lambda^0)}{k_B T^2} \vec{v}_\lambda \otimes \vec{v}_\lambda \tau_\lambda. \tag{A32}$$

By introducing mode heat capacity this transforms into well-known expression (omitting the state indexes)

$$\bar{k}_{ij} = \sum_\lambda C_v v_i v_j \tau. \tag{A33}$$

A connection can be established between the relaxation-time approximation and the iterative technique described earlier. A little algebra shows that the thermal conductivity from Eq. (A32) is identical to the thermal conductivity obtained from the first iteration step of Eqs. (A17) and (A20). That is, the first step of the iterative procedure yields the relaxation-time-approximation result.

APPENDIX B: APPLICATION TO PHONONS

1. Harmonic approximation

In this section we discuss the application of transport theory to the case of phonons in infinite solids. We start by recalling the BTE from Eq. (A10)

$$-\vec{v}_\lambda \cdot \frac{\partial f_\lambda^0}{\partial T} \nabla T = \frac{1}{k_B T} \sum_{\lambda'\lambda''} \left[(\Phi_\lambda + \Phi_{\lambda'} - \Phi_{\lambda''}) \Lambda_{\lambda\lambda'}^{\lambda''} + \frac{1}{2} (\Phi_\lambda - \Phi_{\lambda'} - \Phi_{\lambda''}) \Lambda_\lambda^{\lambda'\lambda''} \right]. \tag{B1}$$

Here the parameters that need to be calculated are the equilibrium transition rates Λ. From the standard harmonic approximation, phonon frequencies and eigenvectors are determined by the eigenvalue equation

$$\sum_J (M_I^{-1/2} M_J^{-1/2} \bar{A}_{IJ;\vec{k}} - \omega_{\vec{k};n}^2 \delta_{IJ}) \vec{e}_{J;\vec{k};n} = 0, \tag{B2}$$

where the dynamical matrix A is defined as

$$\bar{A}_{IJ;\vec{k}} = \sum_{l} \left. \frac{\partial^2 E}{\partial \vec{R}_{I;0}\, \partial \vec{R}_{J;l}} \right|_{\vec{R}^0_{I;0},\vec{R}^0_{J;l}} e^{-i\vec{k}\vec{R}_l}. \tag{B3}$$

In this expression symbols $I,J,\ldots$ represent atomic indices within the elementary cell of the crystal ($I=1,\ldots,N$, where N is the number of atoms in the elementary cell), while $l,l',\ldots$ run over all the cells in the system, and a summation over all repeated indices is implicit. $\vec{R}^0_{I;l}$ represents the equilibrium positions of the atoms.

Limiting ourselves to the quadratic terms in the energy expression, we arrive at the picture of the ideal gas of bosons, i.e., the noninteracting phonons in the solid. Naturally, a solid of this type would have an infinite thermal conductivity since phonons would propagate and carry energy without any interruption. The cubic and higher terms introduce interactions among phonon states (which is the same as to say that phonons are no longer eigenstates of the system), leading to the final intrinsic thermal conductivity of the solids. Indeed, if these higher order terms are sufficiently large, the harmonic approximation becomes much less useful; in particular, the concepts of the wavevector and polarization begin to lose their meanings. This is the situation in amorphous materials[23] and strongly chemically disordered materials. However, for most crystalline systems, the influence of the higher order terms in the energy expansion might be described in terms of modifications of the phonons states. Rather than being represented as a δ function in the density of states, each phonon now represented by a peak of the finite width at some shifted frequency. Higher order terms in the energy expansion contribute to these frequency shifts and phonon widths. Formal expansion is in powers of the ratio of mean-square displacement to the interatomic distance:[17] $\Delta = \sqrt{\langle \Delta x^2 \rangle}/R$. The leading term for the frequency shifts contain contributions from the square of the cubic term and the fourth-order term in the energy expansion, while the leading term for the phonon widths contain square of the cubic term only. For example, in solid argon, $\Delta \sim 0.2$ near the melting temperature of 80 K:[4] hence higher orders might have an effect of $\sim 20\%$ compare to the cubic term. Here we will consider the cubic term in the energy expression only; this is the largest contributor to the finite thermal conductivity.

It is convenient to represent the cubic term in the solid Hamiltonian H_p in terms of suitably defined creation and annihilation phonon operators

$$H_p = \frac{1}{6}\frac{1}{V^{1/2}} \sum_{IJK,\vec{k}\vec{k}'\vec{k}''} \bar{B}_{IJK;\vec{k}\vec{k}'\vec{k}''} \vec{x}_{I;\vec{k}} \vec{x}_{J;\vec{k}'} \vec{x}_{K;\vec{k}''} = \frac{1}{6}\frac{1}{V^{1/2}} \sum_{IJK,\vec{k}\vec{k}'\vec{k}''} \frac{\bar{B}_{IJK;\vec{k}\vec{k}'\vec{k}''}}{m_I^{1/2} m_J^{1/2} m_K^{1/2}} \sum_{nn'n''} \vec{e}^{\,*}_{I;\vec{k};n} \vec{e}^{\,*}_{I;\vec{k}';n'} \vec{e}^{\,*}_{I;\vec{k}'';n''} x'_{\vec{k};n} x'_{\vec{k}';n'} x'_{\vec{k}'';n''}$$

$$= \frac{1}{6} \sum_{nn'n'',\vec{k}\vec{k}'\vec{k}''} \Gamma_{nn'n'';\vec{k}\vec{k}'\vec{k}''} (a^*_{\vec{k};n} - a_{-\vec{k};n})(a^*_{\vec{k}';n'} - a_{-\vec{k}';n'})(a^*_{\vec{k}'';n''} - a_{-\vec{k}'';n''}),$$

$$\Gamma_{nn'n'';\vec{k}\vec{k}'\vec{k}''} = i\frac{(\hbar/2)^{3/2}}{V^{1/2}} \omega^{-1/2}_{\vec{k};n} \omega^{-1/2}_{\vec{k}';n'} \omega^{-1/2}_{\vec{k}'';n''} \sum_{IJK} \frac{\bar{B}_{IJK;\vec{k}\vec{k}'\vec{k}''}}{m_I^{1/2} m_J^{1/2} m_K^{1/2}} \vec{e}^{\,*}_{I;\vec{k};n} \vec{e}^{\,*}_{J;\vec{k}';n'} \vec{e}^{\,*}_{K;\vec{k}'';n''} \tag{B4}$$

in this expression B is a Fourier transform of the third-order force-constant matrix

$$\bar{B}_{IJK;\vec{k}\vec{k}'\vec{k}''} = \delta_{q,\vec{k}+\vec{k}'+\vec{k}''} \sum_{ll'} \left. \frac{\partial^3 E}{\partial \vec{R}_{I;0}\, \partial \vec{R}_{J;l}\, \partial \vec{R}_{K;l'}} \right|_{\vec{R}^0_{I;0},\vec{R}^0_{J;l'},\vec{R}^0_{K;l'}} e^{-i\vec{k}'\vec{R}_l - i\vec{k}''\vec{R}_{l'}}. \tag{B5}$$

By expanding the brackets in the Eq. (B4), we immediately see the possible processes that can take place upon interactions of the phonons

$$H_p = \frac{1}{6} \sum_{nn'n'',\vec{k}\vec{k}'\vec{k}''} \Gamma_{nn'n'';\vec{k}\vec{k}'\vec{k}''} (a^*_{\vec{k};n} - a_{-\vec{k};n})(a^*_{\vec{k}';n'} - a_{-\vec{k}';n'})(a^*_{\vec{k}'';n''} - a_{-\vec{k}'';n''})$$

$$= \frac{1}{6} \sum_{nn'n'',\vec{k}\vec{k}'\vec{k}''} \Gamma_{nn'n'';\vec{k}\vec{k}'\vec{k}''} (a^*_{\vec{k};n} a^*_{\vec{k}';n'} a_{-\vec{k}'';n''} - a^*_{\vec{k};n} a_{-\vec{k}';n'} a^*_{\vec{k}'';n''} + a^*_{\vec{k};n} a_{-\vec{k}';n'} a_{-\vec{k}'';n''} - a_{-\vec{k};n} a^*_{\vec{k}';n'} a^*_{\vec{k}'';n''} + a_{-\vec{k};n} a^*_{\vec{k}';n} a_{-\vec{k}'';n''}$$

$$+ a_{-\vec{k};n} a_{-\vec{k}';n'} a^*_{\vec{k}'';n''}). \tag{B6}$$

Each term describes a specific three-phonon process. For example, the first term describes the process in which a phonon in the mode n'' with the momentum $-\vec{k}''$ splits into the two phonons with the modes n and n', and k vectors $\vec{k}$ and $\vec{k}'$. Notice that Eq. (B6) does not include any terms with three creation operators or annihilation operators, as they would violate energy and momentum conservation. The transition rate between initial state $|i\rangle$ and final state $|f\rangle$ due any of these processes can be described by the Fermi golden rule as[22]

$$P_{if} = \frac{2\pi}{\hbar}\langle f|H_p|i\rangle^2 \delta(E_f - E_i). \tag{B7}$$

Let us consider the first term in Eq. (B6) again. If the initial state for this process $\vec{k};n$, $\vec{k}';n'$, and $-\vec{k}'';n''$ have occupation numbers $n_{\vec{k};n}$, $n_{\vec{k}';n'}$, and $n_{-\vec{k}'';n''}$, then in the final states they are $n_{\vec{k};n}+1$, $n_{\vec{k}';n'}+1$, and $n_{-\vec{k}'';n''}-1$. Any other combinations of the initial and final states will produce zero matrix element due to the orthonormality of the eigenstates. As a result, we obtain

$$\begin{aligned}\langle f|H_p|i\rangle^2 &= \langle n_{\vec{k};n}+1, n_{\vec{k}';n'}+1, n_{-\vec{k}'';n''} \\ &\quad -1|\Gamma_{nn'n'';\vec{k}\vec{k}'\vec{k}''} a^*_{\vec{k};n} a^*_{\vec{k}';n'} a_{-\vec{k}'';n''}|n_{\vec{k};n}, n_{\vec{k}';n'}, n_{\vec{k}'';n''}\rangle^2 \\ &= (n_{\vec{k};n}+1)(n_{\vec{k}';n'}+1) n_{-\vec{k}'';n''} \Gamma^2_{nn'n'';\vec{k}\vec{k}'\vec{k}''}. \end{aligned} \tag{B8}$$

In the case of a thermal system, the average number of phonons in the given state is described by the distribution function $f_{\vec{k};n}$ (note that state is described by k-vector index $\vec{k}$ and branch index n as oppose to generic state index λ that we used in Appendix A). We therefore arrive at the following expression for the transition rate:

$$\begin{aligned}P_{if} = \frac{2\pi}{\hbar}\Gamma^2_{nn'n'';\vec{k}\vec{k}'\vec{k}''}(f_{\vec{k};n}+1)(f_{\vec{k}';n'}+1) f_{-\vec{k}'';n''} \delta(\hbar\omega_{\vec{k};n} \\ + \hbar\omega_{\vec{k}';n'} - \hbar\omega_{-\vec{k}'';n''}). \end{aligned} \tag{B9}$$

By comparing this to Eq. (A5), we identify this contribution with the second term in Eq. (A5). By inspection of Eq. (B6) we can identify the rest of the terms in Eq. (A5). Hence, equilibrium transition rates Λ are given by

$$\begin{aligned}\Lambda^{\vec{k}'';n''}_{\vec{k};n\vec{k}';n'} = \frac{2\pi}{\hbar}\Gamma^2_{nn'n'';\vec{k}\vec{k}'\vec{k}''} f^0_{\vec{k};n} f^0_{\vec{k}';n'} (f^0_{-\vec{k}'';n''}+1)\delta(\hbar\omega_{\vec{k};n} \\ + \hbar\omega_{\vec{k}';n'} - \hbar\omega_{-\vec{k}'';n''}), \end{aligned}$$

$$\begin{aligned}\Lambda^{\vec{k}'';n''\vec{k}';n'}_{\vec{k};n} = \frac{2\pi}{\hbar}\Gamma^2_{nn'n'';\vec{k}\vec{k}'\vec{k}''} f^0_{\vec{k};n} (f^0_{-\vec{k}';n'}+1)(f^0_{-\vec{k}'';n''}+1)\delta(\hbar\omega_{\vec{k};n} \\ + \hbar\omega_{-\vec{k}';n'} - \hbar\omega_{-\vec{k}'';n''}). \end{aligned} \tag{B10}$$

These are the only expressions that are required for the solution of the BTE by the iterative approach and relaxation time approximation. For the variational solution one needs, in addition, to establish the properties, Eq. (A22), of the operator P, representing the right-hand side of the BTE in the case of phonons.

The symmetry properties of the transition probabilities are easily verifiable from the properties of the Bose-Einstein distribution

$$\Lambda^{\lambda''}_{\lambda\lambda'} = \Lambda^{\lambda''}_{\lambda'\lambda}, \quad \Lambda^{\lambda''}_{\lambda\lambda'} = \Lambda^{\lambda\lambda'}_{\lambda''}, \tag{B11}$$

which in turn allows us to establish the properties of Eq. (A22): positive definiteness and symmetry. Writing down the scalar product

$$\begin{aligned}\langle \Psi, P\Phi\rangle &= \frac{1}{k_B T}\sum_{\lambda\lambda'\lambda''} \Psi_\lambda \left[(\Phi_\lambda + \Phi_{\lambda'} - \Phi_{\lambda''})\Lambda^{\lambda''}_{\lambda\lambda'} + \frac{1}{2}(\Phi_\lambda - \Phi_{\lambda'} - \Phi_{\lambda''})\Lambda^{\lambda'\lambda''}_{\lambda} \right] \\ &= \frac{1}{k_B T}\sum_{\lambda\lambda'\lambda''} \Psi_\lambda [(\Phi_\lambda + \Phi_{\lambda'} - \Phi_{\lambda''})\Lambda^{\lambda''}_{\lambda\lambda'}] + \frac{1}{k_B T}\sum_{\lambda\lambda'\lambda''} \Psi_{\lambda''} \left[\frac{1}{2}(\Phi_{\lambda''} - \Phi_{\lambda'} - \Phi_\lambda)\Lambda^{\lambda'\lambda}_{\lambda''} \right] \\ &= \frac{1}{2k_B T}\sum_{\lambda\lambda'\lambda''} \{\Psi_\lambda [(\Phi_\lambda + \Phi_{\lambda'} - \Phi_{\lambda''})\Lambda^{\lambda''}_{\lambda\lambda'}] + \Psi_{\lambda'} [(\Phi_{\lambda'} + \Phi_\lambda - \Phi_{\lambda''})\Lambda^{\lambda''}_{\lambda'\lambda}] - \Psi_{\lambda''} [(\Phi_\lambda + \Phi_{\lambda'} - \Phi_{\lambda''})\Lambda^{\lambda\lambda'}_{\lambda''}]\} \\ &= \frac{1}{2k_B T}\sum_{\lambda\lambda'\lambda''} [(\Psi_\lambda + \Psi_{\lambda'} - \Psi_{\lambda''})\Lambda^{\lambda''}_{\lambda\lambda'}(\Phi_\lambda + \Phi_{\lambda'} - \Phi_{\lambda''})], \end{aligned} \tag{B12}$$

where we have relabeled the summation index in the second line $\lambda \leftrightarrow \lambda''$, split the first term into two while relabeling indexes $\lambda \leftrightarrow \lambda'$ in the third line, and used the symmetries of Λ to arrive at the final expression. From this expression it is obvious that properties of Eq. (A22) are satisfied. This expression is actually used for the numerical calculations in the variational solution as well since it is requires the calculation of only one $\Lambda^{\lambda''}_{\lambda\lambda'}$.

APPENDIX C: IMPLEMENTATION AND TECHNICAL DETAILS

Here we describe the details of numerical calculations involved in the implementation of the three methods. We begin with a discussion of the kind of calculations that are actually involved. Also, we concentrate on the variational principle since it is somewhat easier to describe; all the machinery is directly applicable in the iterative solution and relaxation-time approximation with only a few modifications. As we learned from Appendix A, the three-phonon contribution to the thermal conductivity can be approximated as

$$\begin{aligned}\frac{1}{k} &= \frac{1}{T}\min \frac{\langle \Phi, P\Phi\rangle}{\langle \Phi, X\rangle^2|_{\nabla T=1}} \\ &= \frac{\frac{1}{2k_B T^2}\sum_{\lambda\lambda'\lambda''} [(\Phi_\lambda + \Phi_{\lambda'} - \Phi_{\lambda''})^2 \Lambda^{\lambda''}_{\lambda\lambda'}]}{\left(\sum_\lambda \vec{v}_\lambda \cdot \frac{\partial f^0_\lambda}{\partial T} \nabla T \Phi_\lambda\right)^2}. \end{aligned} \tag{C1}$$

The state index in the phonons case is represented by

$\vec{k}$ vector and branch index n. Summation over the k vectors therefore is substituted by the integration over first Brillouin zone according to the standard recipe. The replacement of the sum by an integration leads to a multiplicative factor of $8\pi^3\hbar^3/V$, where V is the volume

$$\frac{1}{k} = \frac{1}{2k_B T^2} \frac{8\pi^3\hbar^3}{V} \min \frac{\int\int\int \sum_{nn'n''} [(\Phi_{\vec{k};n} + \Phi_{\vec{k}';n'} - \Phi_{\vec{k}'';n''})^2 \Lambda^{\vec{k}'';n''}_{\vec{k};n\vec{k}';n'}] d\vec{k} d\vec{k}' d\vec{k}''}{\left(\int \sum_n \vec{v}_{\vec{k};n} \cdot \frac{\partial f^0_{\vec{k};n}}{\partial T} \nabla T \Phi_{\vec{k};n} d\vec{k} \right)^2}. \tag{C2}$$

The complicated shape of the first Brillouin zone for general lattices makes the evaluation of these integrals difficult. However, it is considerably simple for the orthorhombic, tetragonal, and cubic primitive cells that we discuss below.

Calculations begin with the solution of the usual phonon problem in the first Brillouin zone on a k-point mesh. For the choices of primitive unit cells above, a simple orthogonal mesh will suffice. An odd number of nodes in each direction is used since for such a mesh the sum of coordinates of any two points is a coordinate of another point on the mesh. This is important for the handling of the k-vector δ function that enters Eq. (C2). The k-dependent lattice sums of Eqs. (B3) and (B5) are calculated using previously calculated and stored real space second- and third-order dynamical matrices. The second-order matrices are diagonalized in order to obtain the phonon frequencies and eigenvectors; the group velocities are the calculated by the numerical differentiation. With the choice of the trial function we are now ready to calculate integrals in Eq. (C2).

Triple integration over the Brillouin zone is reduced to double integration by the presence of the δ function that represents momentum conservation. We therefore must perform "only" six-dimensional (6D) integration. The δ function that is responsible for the conservation of energy reduces it to five-dimensional (5D). While handling the first δ function is relatively straightforward, the energy δ function requires considerable care. Two different methods have been proposed in the literature for use in the numerical calculations. One is to substitute some representation of the δ function (Gaussian, or Lorentzian, for example) and perform 6D integration.[23,24] While simple in implementation, reliable results from this method should not depend on the width of the δ-function representation. To achieve this, very fine integration meshes must be used, which are very time consuming. An interesting approach was used by Turney *et al.*,[4] where the width of the δ-function representation was a k-dependent quantity, determined in a self-consistent matter. An alternative method is to reduce the integration to the 5D by analytically evaluating the δ function[5]

$$\int\int\int \delta_{\hbar\omega_{\vec{k};n}+\hbar\omega_{\vec{k}';n'}-\hbar\omega_{\vec{k}'';n''}} dk'_x dk'_y dk'_z = \int\int\int \delta_E dS' dk'_\perp = \int\int\int \delta_E dS' \frac{dk'_\perp}{dE} dE = \int\int\int \delta_E dS' \frac{dE}{\hbar|v|} = \int\int \frac{dS'}{\hbar|v|}$$
$$= \int\int \frac{|v| dk'_x dk'_y}{\hbar |v_z| |v|} = \int\int \frac{dk'_x dk'_y}{\hbar |v_z|},$$

$$E = \hbar\omega_{\vec{k};n} + \hbar\omega_{\vec{k}';n'} - \hbar\omega_{\vec{k}'';n''}, v = \frac{\nabla E}{\hbar} = \frac{1}{\hbar}\left(\frac{\partial E}{\partial k'_x}, \frac{\partial E}{\partial k'_y}, \frac{\partial E}{\partial k'_z} \right). \tag{C3}$$

The difficulty in this case is that domain of integration now is a surface in the k space, called the energy surface, the locations of which needs to be identified. The following method due to Pettersson[7,8,10] is able to do this. For a given k_x and k_y coordinates, the energy argument in the δ function is scanned along the k_z direction. A change in sign signifies the surface position; linear interpolation is then used to determine the precise crossing point. The group velocity vector at this point indicates the orientation of the surface [from Eq. (C3)] and allows us to calculate its area (with the restriction that it must belong to the integration domain, i.e., the first Brillouin zone). The value of the integrand also has to be

evaluated at this crossing k point. The integrand includes the eigenvalues, eigenvectors and the Fourier transform of the third order dynamical matrix. An important issue is that position of the surface in general will not coincide with the k-point mesh used for the calculations. Moreover, it is possible that when comparing the energies at two neighboring k points a branch crossing had occurred somewhere in between or that there is a degenerate eigenstate at one or both of those k points. In these cases one would use incorrect eigenvalue/eigenvector pair in the calculations. Using the wrong eigenvectors will significantly alter the results of the calculations. In order to avoid such a mismatch, perturbation theory calculations are performed for every k point with the change in dynamical matrix produced by the small displacements along k_z as a perturbation

$$\begin{aligned} M_I^{-1/2}M_J^{-1/2}\bar{A}_{IJ;\vec{k}} &= M_I^{-1/2}M_J^{-1/2}\sum_l \bar{A}_{IJ;l}e^{-i\vec{k}\vec{R}_l} \\ &= M_I^{-1/2}M_J^{-1/2}\sum_l \bar{A}_{IJ;l}e^{-i(\vec{k}_0+\Delta k_z)\vec{R}_l} \\ &= M_I^{-1/2}M_J^{-1/2}\Bigg\{\sum_l \bar{A}_{IJ;l}e^{-i\vec{k}_0\vec{R}_l} - \Delta k_z\sum_l \bar{A}_{IJ;l}R_{zl} \\ &\quad + \frac{1}{2}\Delta k_z^2\sum_l \bar{A}_{IJ;l}R_{zl}^2 + \cdots\Bigg\} \\ &= M_I^{-1/2}M_J^{-1/2}\bar{A}_{IJ;\vec{k}_0} + \Delta k_z\bar{D}_{IJ}^1 + \Delta k_z^2\bar{D}_{IJ}^2. \end{aligned} \quad \text{(C4)}$$

The quadratic term is included since in some cases the first term is identically zero due to symmetry of the crystal. First-order perturbation theory then provides the correction to the eigenvalues

$$\omega_{\vec{k},n}^2 = \omega_{\vec{k}_0,n}^2 + \Delta k_z\vec{e}_{I;\vec{k}_0;n}^*\bar{D}_{IJ}^1\vec{e}_{J;\vec{k}_0;n} + \Delta k_z^2\vec{e}_{I;\vec{k}_0;n}^*\bar{D}_{IJ}^2\vec{e}_{J;\vec{k}_0;n}, \quad \text{(C5)}$$

where again, the second term is taken into account only if first one is identically zero. Correction to the eigenvectors appears only if the initial state is degenerate and represents rotation in the degenerate subspace. A detailed description of this procedure can be found in many quantum-mechanics textbooks.[22] The last step needed in order to guarantee a proper eigenvalue/eigenstate pair is to resort the corrected eigenvalues (and eigenvectors) in ascending order and use the eigenvalue with the original branch index for the integrand calculation. Figure 5 illustrates the whole procedure on the example of two states: while scanning state 1, there will be no crossing of the energy surface detected.

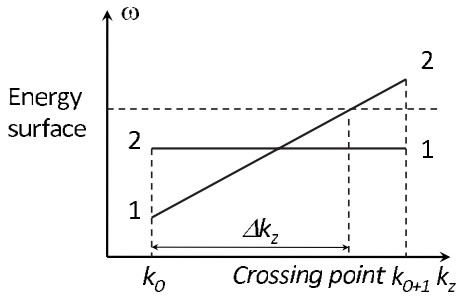

FIG. 5. Illustration of the perturbation theory calculations if two states crossed near the energy surface.

Going along state 2 in Fig. 5, a crossing will be detected. However, at point k_0 the order of the states is reversed, compare to the order at the crossing point. Performing a perturbation calculation will change the magnitude of the eigenvalues, while resorting them will put them in correct order. From Fig. 5 one can also see that next grid point k_{0+1} can also be considered as a starting point of the calculations, going into negative direction along z axis. In fact, we perform calculations at both of these points and average out the result with the proper weight.

These calculations take a fairly small amount of time because for every k point the correction to the eigenvalues can be precalculated up to displacement factor and because degenerate eigenvectors can be rotated in advance. Therefore, once the position of the energy surface is identified and Δk_z is known, one just need multiply the correction by it and resort eigenvalues. Finally, in order to increase accuracy of the calculations, additional fine gridding is used along z direction only. These additional points are not treated as an integration points; rather this fine gridding allows for the precise determination of the integration surface. The results presented in the body of the paper illustrate this point.

*Corresponding author; alextch@gmail.com

[1] P. K. Schelling, S. R. Phillpot, and P. Keblinski, Phys. Rev. B **65**, 144306 (2002).
[2] X. Gonze and J. Vigneron, Phys. Rev. B **39**, 13120 (1989).
[3] P. G. Klemens, Solid State Phys. **7**, 1 (1958).
[4] J. E. Turney, E. S. Landry, A. J. H. McGaughey, and C. H. Amon, Phys. Rev. B **79**, 064301 (2009).
[5] J. M. Ziman, *Electrons and Phonons* (Clarendon Press, Oxford, 1962).
[6] D. Benin, Phys. Rev. B **1**, 2777 (1970).
[7] S. Pettersson, J. Phys. C **20**, 1047 (1987).
[8] S. Pettersson, Phys. Rev. B **43**, 9238 (1991).
[9] M. Omini and A. Sparavigna, Physica B **212**, 101 (1995).
[10] D. A. Broido, A. Ward, and N. Mingo, Phys. Rev. B **72**, 014308 (2005).
[11] K. V. Tretiakov and S. Scandolo, J. Chem. Phys. **120**, 3765 (2004).
[12] Y. Chen, J. R. Lukes, D. Li, J. Yang, and Y. Wu, J. Chem. Phys. **120**, 3841 (2004).
[13] A. J. H. McGaughey and M. Kaviany, Int. J. Heat Mass Transfer **47**, 1783 (2004).
[14] H. Kaburaki, J. Li, and S. Yip, Mater. Res. Soc. Symp. Proc. **538**, 503 (1999).
[15] H. Kaburaki, J. Li, S. Yip, and H. Kimizuka, J. Appl. Phys. **102**,

043514 (2007).
[16] A. A. Maradudin and A. E. Fein, Phys. Rev. **128**, 2589 (1962).
[17] G. K. Horton and E. R. Cowley, *Physics of Phonons* (Springer, Berlin, 1987).
[18] F. Clayton, D. N. Batchelder, J. Phys. C **6**, 1213 (1973).
[19] A. Chernatynskiy, J. E. Turney, A. J. H. McGaughey, and S. R. Phillpot (unpublished).
[20] B. M. Askerov, *Electron Transport Phenomena in Semiconductors* (World Scientific, Singapore, 1994).
[21] O. Axelsson, *Iterative Solution Methods* (Cambridge University Press, Cambridge, 1996).
[22] D. J. Griffiths, *Introduction to Quantum Mechanics* (Prentice Hall, Englewood Cliffs, 1994).
[23] P. B. Allen, J. L. Feldman, J. Fabian, and F. Wooten, Philos. Mag. B **79**, 1715 (1999).
[24] A. J. C. Ladd, B. Moran, and W. G. Hoover, Phys. Rev. B **34**, 5058 (1986).